The Save-the-Rhino Antenna: A Horn-Mounted Wire-Based Monopole

Guy A. E. Vandenbosch, Jiahao Zhang, Sen Yan, and Vladimir Volski

***Abstract*—A new antenna topology dedicated to being mounted on the horn of an adult rhino is proposed. The curved topology of the horn, the material characteristics of the horn material, mechanical aspects when being mounted, and the typical behavior of rhinos in the wild are taken into account in the design process. The results are extremely promising. It is illustrated that this antenna is much better than antennas already operational in tracking networks targeting rhinos. In this way, it may contribute to the rescue of this endangered species.**

***Index Terms*—Anti-poaching, on-animal tracking antenna, rhinoceros, wireless sensor network.**

I. Introduction

FROM 2007 to 2017, the number of poached rhinos increased spectacularly. In the most recent years, every year more than 1000 rhinos have been shot for their horn. With only about 30 000 individuals left on the planet (approximately 25 000 on the African continent), this means that every year about 3% of the worldwide rhino population is killed [1]. The largest markets for rhino horn are Vietnam and China. There are two main uses for the horn. First, in traditional medicine in these countries it forms a remedy against several diseases and ailments. Second, it is often used as a collectable and symbol of great wealth and prestige. Because of the large demand and the ban from official markets, the price per kg (50 000–100 000 dollar/kg) is higher than for gold [2], [3].

Numerous measures have already been taken. In general, it is hugely important that poachers are caught on-site so that they can be effectively prosecuted. Some research groups in South Africa have tried to assist the park rangers by developing on-animal transmitter systems to send the locations of the rhinos or a distress signal to the nodes of a wireless network. First, the patrol routes can then be optimized in real time based on the location data. Second, poachers can be caught in the act when the network picks up something unusual.

The transmitter that is currently in use in South Africa is fixed at the ankle of the rhino, which is sometimes as low as 0.1 m above the ground. However, since the rhino living environment mainly consists of low vegetation, height differences, rocks, etc., the propagational environment is extremely harsh. An on-animal transmitting antenna that is located higher up on the animal, for example, on the horn, would be able to boost the performance of the network considerably. This solution has already been implemented about 30 years ago [4], [5], but without any attempt to develop a dedicated antenna for this purpose. Since the antenna as such was not the topic of these works, it is very well possible that the presence of the horn had a destructive effect on the matching of the antenna there.

The design of a dedicated antenna, fully taking into account the presence of the horn and the effect on its characteristics, is the main innovation in this work. Designing such an antenna includes several difficult challenges, such as the making of a correct electromagnetic model (EM model) for the rhino horn, the design of a suited topology to be mounted on the horn, mechanical stability and durability, also during the normal daily activities of the rhinos. Rhinos mostly use their horn to push aside vegetation, rocks, etc., when grazing. Very rarely they must defend themselves against other large animals or predators. In this case, the horn is used a lot and must endure large mechanical stress [6].

II. Horn Model

A. Dielectric Properties

Unlike most animal horns, the core of the rhino horn is not made up of bone. Instead, it has a core consisting of melanin and calcium phosphate salt that provides mechanical strength and protection against UV radiation. The outer layer of the horn consists out of keratin, which is a protein originating from dying cells. The result is a very water-resistant and hard material [7]. The process of keratinization only occurs at the very bottom of the horn. The pointy shape and the curvature are actually an effect of the wear and tear over time. Therefore, the top part of the horn always is the oldest [7]. When mounting an antenna on a rhino horn, the horn will have a great influence on the antenna characteristics. Therefore, it is very important to have an accurate image of the dielectric properties of the horn.

In the existing literature, the following ranges for the real part of the permittivity are found: keratin: $3 \rightarrow 7$ [8], [9]; melanin: $7 \rightarrow 10$ [10]; calcium phosphate salt: $22 \rightarrow 23$ [11]. In order to establish a suitable reference horn model, the first estimation concerns the mix between the melanin and the calcium phosphate salt. It is assumed that one-third of the core is melanin and the other two-thirds is calcium phosphate salt. This delivers an effective core relative permittivity of

$$\varepsilon'_{\text{core}} = \frac{1}{3}\varepsilon'_{\text{melanin}} + \frac{2}{3}\varepsilon'_{CaP} \approx 17. \quad (1)$$

Manuscript received December 23, 2021; revised January 31, 2022; accepted February 5, 2022. Date of publication February 14, 2022; date of current version May 5, 2022. *(Corresponding author: Vladimir Volski.)*

Guy A. E. Vandenbosch and Vladimir Volski are with the Department of Electrical Engineering, Division ESAT-WaveCoRE, Katholieke Universiteit Leuven, 3001 Leuven, Belgium (e-mail: guy.vandenbosch@kuleuven.be; vladimir.volski@esat.kuleuven.be).

Jiahao Zhang is with the National Key Laboratory of Science and Technology on Vessel Integrated Power System, Naval University of Engineering, Wuhan 430033, China (e-mail: jiahao.z@hotmail.com).

Sen Yan is with the School of Information and Communications Engineering, Xi'an Jiaotong University, Xi'an 710049, China (e-mail: sen.yan@xjtu.edu.cn).

Digital Object Identifier 10.1109/LAWP.2022.3151215

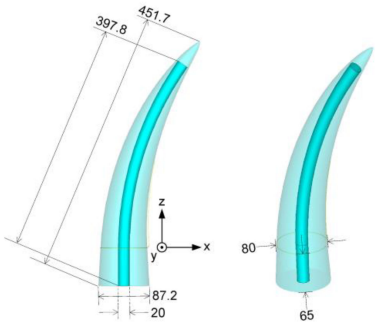

Fig. 1. Topology of the rhino horn model used in the design: side view and perspective view. The curvature radius of the horn axis is 500 mm; see also Fig. 4.

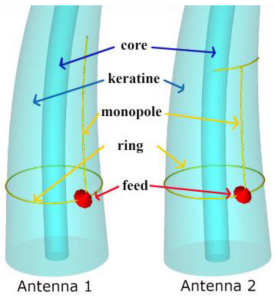

Fig. 2. Topology of the Antenna 1 (left) and Antenna 2 (right).

Note that in the design phase (see Section III) the sensitivity of our design to this value was checked by also simulating the characteristics of models with a core permittivity of 15 and 22, respectively. It turns out that this sensitivity is acceptable for the design, which is due to the fact that the core of the horn is further away from the antenna. The permittivity of keratin was proven to be much more important to the antenna behavior. In a similar way, simulations were performed with the permittivity of keratin in the range $3 \rightarrow 7$. The optimal results, i.e., the best agreements between simulations and measurements were obtained with a value of 3. In the rest of this letter, this value is thus taken as the relative permittivity of keratin. For the imaginary part of the permittivity, the values found in the literature were $\varepsilon''_{\text{core}} = 0.02$ and $\varepsilon''_{\text{keratin}} = 0.08$ [8]–[11].

B. Topology

In real life the horn of a rhino continuously changes. It changes by growing, being damaged, breaking off, or—the worst—by being cut off. In order to design an antenna for rhino horns, a reference horn topology is necessary. Such a topology was selected based on a visual study of typical adult rhino horns. The result is depicted in Fig. 1. It has to be emphasized that the precise structure of the horn at the tip and bottom is less important than the structure in the region where the antenna will be mounted (see also Fig. 2). This allows to simplify the topological model that will be used in the computational tools.

III. Antenna Design

Based on the wireless network used and on the way the horn is averagely positioned in the daily life of a rhino, specifications can be deduced for the antenna to be mounted on it. The network currently used operates at 433 MHz. The antenna currently used at the ankle inside a transmitter box has a bandwidth of 8.4 MHz [12]. As the antenna must serve in a tracking network, the radiation pattern should be near to omnidirectional in the horizontal plane. From a mechanical point of view, the use of simple metal wire of a thick enough diameter and mounted at the back of the horn satisfies the requirements. Positioning it there minimizes the mechanical stress due to natural animal behavior. Based on these considerations, two topologies were selected and two corresponding antennas were designed and optimized. The designs and optimizations were performed with CST Microwave Studio. Both antennas used noninsulated copper wire with a diameter of 0.6 mm.

TABLE I
Dimensions of Antennas 1 and 2

	Antenna 1	Antenna 2
Ground ring radius	40 mm	40 mm
Length monopole	150 mm	110 mm
Radius upper ring	/	35 mm
Total length upper ring	/	45 mm

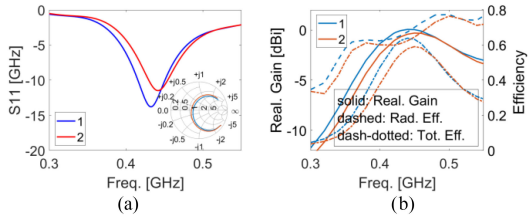

Fig. 3. Simulated results of Antennas 1 and 2. (a) *S*-parameters. (b) Realized gain and efficiency.

The first topology consists of a ring of radius $a = 40$ mm that can be fixed around the horn, which can be seen as forming the small ground for a quarter wavelength monopole type arm that follows the curvature of the horn. Another way of looking at this structure is to consider the ring as a bifurcated second arm of a noncenter fed and curved dipole. Of course, the antenna functioning of the structure is not depending on this point of view, just on the way the currents are flowing on the metal wires. Although a quarter wavelength at 433 MHz is 173 mm, the final length of the monopole arm is smaller because the antenna has to be mounted on a high permittivity material. An optimization targeting the best matching at this frequency delivered 150 mm (0.22 λ at 433 MHz). This antenna will be referred to as "Antenna 1."

The second topology is based on the first one. It connects two extra wires to the top of the monopole arm that form a partial ring going around the horn. This offers the possibility to increase the mechanical strength of the antenna. With a fixed radius of 40 mm for the ground ring and a variable radius for the partial top ring, this antenna also can be fixed on every horn, regardless of its exact shape. In the design, because of the extra wires that go around the horn, the monopole arm length shrinks a bit. An optimization targeting the best matching at 433 MHz delivered a monopole arm length of 110 mm (0.16 λ) and a total length of the partial upper ring of 45 mm (0.065 λ). This antenna will be referred to as "Antenna 2." The physical dimensions of both antennas are summarized in Table I.

The reflection coefficient as well as the realized gain and the antenna efficiency for both antennas is plotted in Fig. 3. Antenna 1 reaches a –10 dB bandwidth of 33 MHz, which is

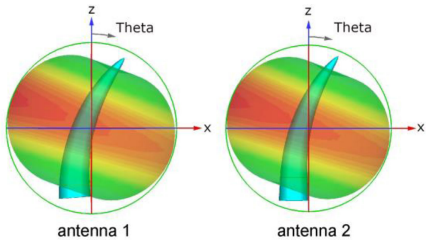

Fig. 4. Simulated radiation pattern of antennas 1 and 2.

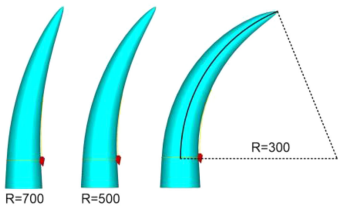

Fig. 5. Curvature robustness. From left to right: curvature radii of 700, 500, and 300 mm, respectively, for antenna 1.

more than 3 times the bandwidth of the ankle mounted antenna used presently by Stellenbosch University. The matching of Antenna 2 is worse. At the center frequency, a reflection coefficient of only –11.5 dB is reached. Note that in order to keep the structure as simple and cheap as possible, no matching network is used. Both antennas show an approximately omnidirectional radiation pattern. The directivity is 2.05 dBi for Antenna 1 and 1.95 dBi for Antenna 2 at the operational frequency and stays more or less constant in the entire bandwidth (see Fig. 4). Realized gains of ca. −0.15 and –0.41 dBi are obtained for Antennas 1 and 2, respectively. The main reason for the lower gain is the reduced radiation efficiency due to the losses inside the rhino horn. Note that the maximal directivity is reached in the direction to the front side of the horn, while the antenna is located at the back side of the horn.

IV. Antenna Robustness

Because of the fact that extra mechanical strength can also be provided using small nonconducting straps placed around the horn (see for example Fig. 10), antenna 1, which shows the best results, is selected for further investigation. Since first of all, different horns obviously have a different topology, and second, even for the same horn the horn-mounted antenna will not remain static in nature due to the daily activities of the rhino, a numerical sensitivity analysis has been executed with CST Microwave Studio.

The influence of the horn curvature (see Fig. 5), the ring shape, the keratin losses, and the ring size have been investigated. Only a single parameter is varied at the same time. The influence of the horn curvature is almost negligible (see Fig. 6). Also, the effect of the ring shape is very moderate (see Fig. 7). For a constant circumference of the ring, always firmly fixed to the horn without any air gaps, the antenna behavior is not affected significantly. Higher keratin losses yield a slightly larger bandwidth with a slightly better matching (see Fig. 8). The ring size clearly affects the operational frequency band (see Fig. 9). This could be expected, since a different ring shape comes with a different ground wire length. However, the –10 dB band still covers the targeted band. The realized gain also varies slightly.

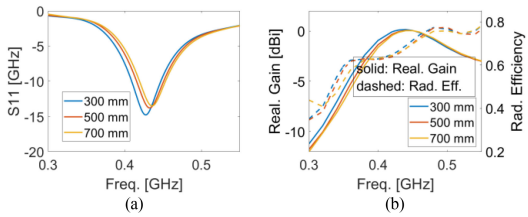

Fig. 6. Curvature robustness for antenna 1. (a) *S*-parameters. (b) Realized gain and radiation efficiency.

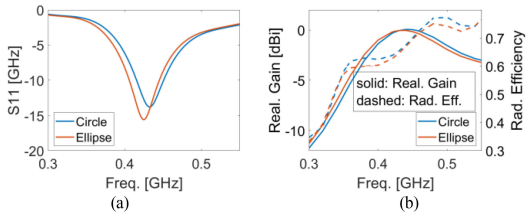

Fig. 7. Ring shape robustness: circular shape (blue), elliptical shape with minor axis / major axis = 0.8 (red), for antenna 1. (a) *S*-parameters. (b) Realized gain and Radiation Efficiency.

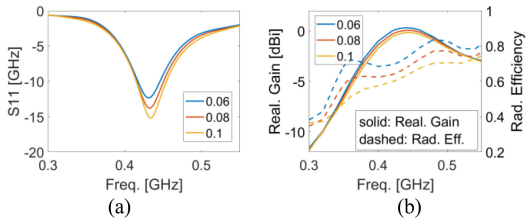

Fig. 8. Keratin losses robustness (different ε"keratin), for antenna 1 (which has curvature 500 mm). (a) *S*-parameters. (b) Realized gain and radiation efficiency.

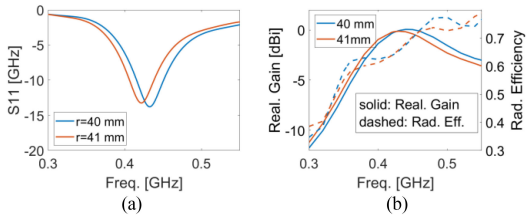

Fig. 9. Ring size robustness for antenna 1. (a) *S*-parameters. (b) Realized gain and radiation efficiency.

V. Measurements

A prototype was fabricated from copper wires in combination with a real rhino horn. The prototype is fed via an SMA connector. The monopole is soldered to the inner pin, and the monopole ring is soldered to the SMA ground conductor. So, the ring mimics the ground. A semi-rigid coaxial cable is connected to the SMA connector, as shown in Fig. 10. Since it is impossible to actually measure on a live rhino, for obvious reasons, the horn was borrowed from a museum (see Fig. 10). The antenna prototype is secured to the horn with elastic rubber bands (nonconductive straps).

The S_{11} parameter of the combination Antenna 1 on horn was measured with a network analyzer. The result is given in Fig. 11. The measured center frequency is 425 MHz, a discrepancy of 8 MHz in comparison with the design frequency of 433 MHz. Because of the wide measured bandwidth of 50 MHz, the operational band is still fully covered, illustrating the good "robustness" of the design. The radiation pattern in

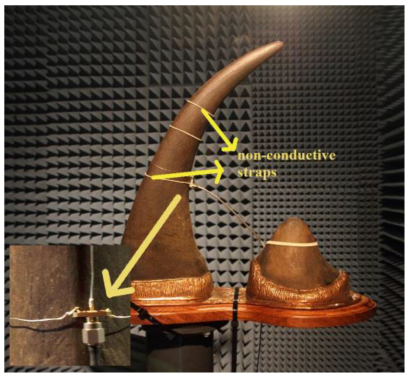

Fig. 10. Rhino horn mounted on a positioner in the anechoic room.

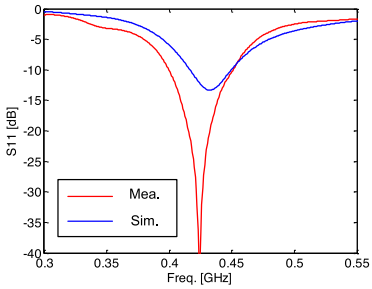

Fig. 11. Measured reflection coefficient for the real horn of Fig. 10 compared to the simulated reflection coefficient of the model in Fig. 1.

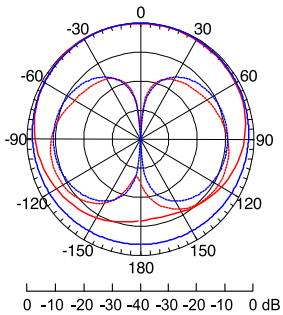

Fig. 12. Far-field pattern in the horizontal plane: simulations (blue, for model in Fig. 1) and measurements (red, for real antenna in Fig. 10), copolarization in solid line, cross polarization in dashed line.

the horizontal plane was measured in the anechoic room at KU Leuven. A biconical reference antenna was used which was fed by a 10 dBm signal.

The normalized copolar and cross-polar radiation patterns are given in Fig. 12. The copolar component is basically omnidirectional in the horizontal plane, as required by the application. In the backward direction, there is a little drop of about 4 dBm in the simulations, and a more severe drop of 12 dBm in the measurements. This discrepancy is mainly due to the parasitic current flowing on the outside of the feeding cable (although ferrites were used to suppress this common mode current). This current contributes to the radiation, depending on the orientation of the feeding cable. In real circumstances, the backward direction is less important, since it is there that the rest of the body of the rhino is located. The cross-polar level is in the order of –10 dB.

In order to investigate the robustness of the radiation pattern when the rhino moves, the normalized radiation patterns in

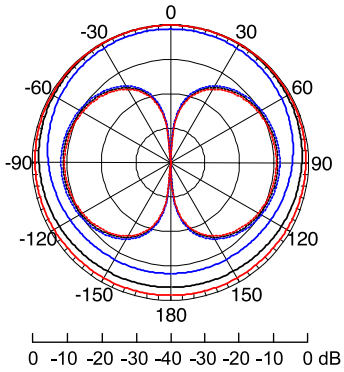

Fig. 13. Radiation patterns in different planes. Black lines: horizontal plane, blue lines: –20° (clockwise direction in Fig. 1), red line: +20° (clockwise direction in Fig. 1), solid lines: copolarization, dashed lines: cross polarization.

different planes are compared and shown in Fig. 13. As we can see, the forward radiation does not change much.

The simulated realized gain at 0.424 GHz is –0.2 dBi. The measured realized gain was calculated based on Friis' transmission equation. The signal generator produced a 10 dBm signal, all cable losses were measured, and the gain of the reference antenna was extracted from its data sheet. The realized gain was then calculated as follows:

$$G_r = \frac{P_r}{P_t G_t}\left(\frac{4\pi d}{\lambda}\right)^2.$$

The result at 0.424 GHz is 0.1 dBi. These gains stay quasi constant in the relatively small operational band of the tracking system.

VI. Practical Considerations

In [4] and [5], for the first time, antennas were incorporated in a rhino horn. However, as far as the authors can see, the antennas used in these papers are the off-the-shelf-antennas that come with the transmitters. They are not dedicated designs, which is the main target of this letter. This can result in a huge difference in performance. The practical methods to incorporate the antenna and transmitter in the horn concern drilling and cutting grooves in the horn. This reassures that the system is rugged enough to allow a normal horn functionality (digging, breaking branches, etc.). It is also wise to locate the antenna and the transmitter close together in the drill holes/grooves in order to avoid common mode currents flowing in a connecting transmission line. For further details, we refer to these papers. Another technique that could be investigated is to use straps, for example, made of very strong carbon fibers.

VII. Conclusion

A dedicated wire antenna was designed to be mounted on the horn of African rhinos within the context of a wireless network to be deployed to stop the poaching of this animal. The measured bandwidth of 50 MHz is large compared to the required bandwidth of 8 MHz, making the design quite robust. The resulting radiation pattern is almost omnidirectional, as required in this application, with a realized gain of ca. 0 dB. Propagational models predict that a transmitter equipped with this antenna can be tracked in an area considerably larger than with the original antenna mounted on the ankle of the rhino.

REFERENCES

[1] Poaching statistics, Apr. 2020. [Online]. Available: www.savetherhino.org

[2] S. Petrus le Roux, "A prototype animal borne behaviour monitoring system," Master's thesis, Dept. Elect. Electron. Eng., Univ. Stellenbosch, Stellenbosch, South Africa, 2016.

[3] Y. Gao, K. J. Stoner, A. T. L. Lee, and S. G. Clark, "Rhino horn trade in China: An analysis of the art and antiques market," *Biol. Conservation*, vol. 201, pp. 343–347, Sep. 2016.

[4] D. J. Pienaar and A. J. Hall-Martin, "Radio transmitter implants in the horns of both the white and the black rhinoceros in the Kruger National Park," *Koedoe*, vol. 34, no. 2, pp. 89–96, 1991.

[5] A. M. Shrader and B. Beauchamp, "A new method for implanting radio transmitters into the horns of black and white rhinoceros," *Pachyderm*, vol. 30, pp. 81–86, Jan.–Jun. 2001.

[6] Rhinos, Apr. 2020. [Online]. Available: Wikipedia.org

[7] T. L. Hieronymus, L. M. Witmer, and R. C. Ridgely, "Structure of white rhinoceros (*Ceratotherium simum*) horn investigated by X-ray computed tomography and histology with implications for growth and external form," *J. Morphol.*, vol. 267, no. 10, pp. 1172–1176, Oct. 2006.

[8] E. Marzec, "Analysis of the dielectric properties of keratin in the alpha-dispersion electric field region," *Med. Biol. Eng. Comput.*, vol. 39, no. 5, pp. 558–561, Sep. 2001.

[9] H. Maeda, "Water in keratin. Piezoelectric, dielectric, and elastic experiments," *Biophys. J.*, vol. 56, no. 5, pp. 861–868, Nov. 1989.

[10] H. Isotalo, M. M. Jastrzebska, and S. Jussila, "Dielectric response and a.c. conductivity of synthetic dopa-melanin polymer," *J. Mater. Sci.*, vol. 33, no. 16, pp. 4023–4028, Aug. 1998.

[11] O. Kaygili S. Keser, T. Ates, S. Kirbag, and F. Yakuphanoglu, "Dielectric properties of calcium phosphate ceramics," *Mater. Sci.*, vol. 22, Feb. 2016, Art. no. 1.

[12] S. C. K. Dodson, P. G. Wiid, and T. R. Niesler, "Design of a folded split ring resonator antenna for use in an animal-borne sensor," in *Proc. IEEE Radio Antenna Days Indian Ocean*, Sep. 2017, pp. 1–2.